Electronic Supplementary Information

Overcoming microbial resuscitation using stable ultrafine gold nanosystems

Anindita Thakur,[a] Pranay Amruth Maroju,[a] Ramakrishnan Ganesan*[b] and Jayati Ray Dutta*[a]

a   Ms. A. Thakur, Mr. P. A. Maroju, Dr. J. R. Dutta*
Department of Biological Sciences
Birla Institute of Technology and Science (BITS), Pilani, Hyderabad Campus
Jawahar Nagar, Kapra Mandal, Medchal District, Hyderabad, Telangana – 500078. India.
E-mail: jayati@hyderabad.bits-pilani.ac.in

b   Dr. R. Ganesan*
Department of Chemistry
Birla Institute of Technology and Science (BITS), Pilani, Hyderabad Campus
Jawahar Nagar, Kapra Mandal, Medchal District, Hyderabad, Telangana – 500078. India
E-mail: ram.ganesan@hyderabad.bits-pilani.ac.in

Contents

Experimental section

Materials

Gold(III) chloride (Au 64.4% min), which is the precursor of the Au NCs, was procured from Alfa-Aesar, whereas the common laboratory reagents like, potassium iodide, potato starch (extra pure) and chloroform (99.5%) were purchased from SD Fine chemicals, India Pvt. Ltd. Microbiology reagents such as sodium thiosulphate anhydrous (99.5%), ampicillin sodium salt, resazurin sodium salt, Luria-Bertani broth (LB broth), Luria-Bertani agar (LB agar), Tris base, ethylenediamine tetraacetic acid (EDTA, >99%), sodium dodecyl sulfate (SDS), sodium chloride (99.9%), potassium chloride and ethidium bromide were procured from Himedia, India Pvt. Ltd. Reagents such as sodium phosphate dibasic dihydrate (99.5%) and potassium dihydrogen orthophosphate (99.5%) were bought from SRL chemicals Pvt. Ltd. Anhydrous citric acid, L-glutathione reduced (GSH, (≥98%)), isopropyl alcohol, sodium hydroxide (≥99%), 2,7-dichlorofluorescein diacetate (DCFH-DA, >97%), 2-mercaptobenzimidazole (2-MBI), phenol and glutaraldehyde were purchased from Sigma Aldrich. Live/Dead BacLight bacterial viability kit was procured from Invitrogen, Thermo fisher Scientific, to stain the cells prior to FACS analyses. SeaKem® LE agarose was obtained from Lonza, while RNAse was procured from Macherey-nagel MN. The RNeasy® mini kit was purchased from Qiagen, TB green® Premix Ex-Taq II (Tli RNaseH Plus), while trizol and cDNA synthesis kit were procured from Takara. Next-Gen DNA ladder was purchased from Puregene, Genetix. The primers used in the reverse transcription-quantitative polymerase chain reaction (RT-qPCR) studies were procured from Eurofins Pvt Ltd.

Characterization

The absorbance and particle size analyses of the as-synthesized Au NCs were initially characterized using UV-visible spectroscopy (Jasco V-650) and dynamic light scattering (DLS, Malvern Zeta sizer), respectively. The UV-visible spectra were obtained at a scan rate of 1000 nm/min. The high-resolution transmission electron microscopy (HR-TEM) images of the as-synthesized Au NCs and ligand-modulated UGNs were obtained using a JEOL (JEM 2100 PLUS) instrument by drop-casting the samples onto a 200-mesh copper TEM grid. X-ray photoelectron spectroscopy (XPS; Thermofisher K-Alpha) was employed to ascertain the reduction of gold (III) chloride in the as-synthesized Au NCs (Fig. S1), wherein an average of 5 scans at three different spots were obtained. Surface site modulation studies of UGNs using different concentrations of 2-MBI were performed using liquid chromatography (Shimadzu LCMS 8040), as per our previously reported protocol.[1] The mercaptan group in 2-MBI is assumed to bind with the surface gold atoms in a 1:1 ratio. The ^{1}H NMR studies of the UGNs with and without GSH-capping were performed using Bruker AV NEO 400 MHz spectroscopy. The fluorescence intensity, to track the performance of the antimicrobials through resazurin assay, was measured using a plate reader (SpectraMax® iD3, Molecular Devices, USA) by employing the excitation and emission wavelengths as 530 nm and 590 nm, respectively. The same instrument was used for ROS estimation but employing the excitation and emission wavelengths as 485 nm and 525 nm, respectively. Fluorescence-activated cell sorter (FACS) studies were carried out using BD FACSAria III Cell Sorter instrument. The percentage gold distribution was performed by measuring the absorbance of the solution at 267.595 nm under nitrogen atmosphere and argon plasma using Prodigy High Dispersion ICP-OES (Teledyne Leeman Labs) instrument. The RT-qPCR experiments were undertaken using Roche 480 LightCycler.

Synthesis of Au NCs, relative surface site modulation and stability studies

Weakly-capped Au NCs were synthesized through a pseudo-solid-state-approach following our previous report.[1] The as-synthesized Au NCs were then subjected to surface ligand modulation as per the following procedure. About 10 mg of the as-synthesized Au NCs was added to 1 mL of an aqueous solution containing 6.25 mg of NaOH (3 equivalent to citric acid) to obtain UGN(-)GSH. In the case of GSH capping, this NaOH solution was additionally containing 0.2, 0.4 or 0.8 mg of GSH to obtain UGN(+)GSH50, UGN(+)GSH100 and UGN(+)GSH200,

respectively. It can be noted that each batch was synthesized taking 150 mg of citric acid, wherein the amount of AuCl$_3$ added was ~6 mg. Thus, for the total batch, the amount of GSH in UGN(+)GSH50, UGN(+)GSH100 and UGN(+)GSH200 samples was 3, 6 and 12 mg, respectively. Since the molar mass values of AuCl$_3$ and GSH are very close, their mass ratio is also assumed to represent the molar ratio.

For characterizing the relative surface site modulation, 30 nmol of 2-MBI probe in 2 mL of methanol and water mixture (1:1 ratio) was incubated for 1 h with 100 μL of UGNs having a concentration of 1.8 mg/mL, following which the solution was centrifuged for 30 min at 13,000 rpm. The supernatant was collected and estimated for the residual 2-MBI concentration using liquid chromatography (LC).

Stability studies were performed using an aqueous solution containing 3 mg/mL concentration of the given UGNs composition. The solutions were subjected to 60 rpm shaking in an orbital shaker up to 48 h, and the absorbance was monitored periodically.

Resazurin assay for inhibitory concentration-50 (IC$_{50}$) determination

About 100 μL of the microbial culture containing a cell density of 10^7 CFU/mL was taken in a 96 well plate, to which 100 μL of an aqueous solution containing varying concentrations of the antimicrobials was added.[2] The final concentration of UGNs in the solutions were ranging from 5 to 55 μg/mL, while that of ampicillin varied from 1 to 95 μM (0.35 to 33.25 μg/mL). The resultant solutions were then incubated for 6 h, after which about 20 μL of 0.02% resazurin dye solution was added to all the seeded cultures along with the blank and control. The fluorescence intensity of the sample solutions was then recorded, which were then normalized with that of the blank. The average of triplicate measurements was presented along with the standard deviation. The value of the antimicrobials corresponding to ~50% inhibition was identified as IC$_{50}$.

Minimum inhibitory concentration (MIC) determination

The MIC of the antimicrobials was determined using the standard broth dilution method. The OD of the overnight culture was measured at 600 nm and the solution was diluted to obtain a cell population of 5×10^5 CFU/mL, from which about 100 μL of the culture was introduced into each well of a 96-well plate. To each well, about 100 μL of the antimicrobial compound was added in different dilutions and then incubated for 18 h at 37 °C. The lowest concentration inhibiting the visible growth—as determined by the absence of any turbidity—of the microbes was considered as the MIC.

Minimum bactericidal concentration (MBC) determination

The MBC of the antimicrobials employed in this study was determined following the standard LB agar plating method. For this, about 100 μL of the bacterial cultures (10^7 CFU/mL) were seeded in a 1.5 mL eppendorf, to which 100 μL of the solutions containing varying concentrations of the antimicrobials were added. The obtained reaction mixtures were incubated for 6 h, following which 10 μL of the solution from each eppendorf was withdrawn and mixed with 20 μL of autoclaved MilliQ water before proceeding with plating. In the time-kill MBC analysis, the initial incubation time for the bacterial cultures with the antimicrobials was varied as 6, 12, 24 and 48 h, after which the aliquots from the cultures were subjected to plating and the colony count was performed after 24 h. The lowest concentration at which no bacterial colony observed was considered as the MBC.

Resuscitation studies

To study the microbial resuscitation, the changes in the OD$_{600}$ were monitored to follow the correlation between microbial growth and the aggregation dynamics of the UGNs. The bacterial viability was also followed using the resazurin assay as per the above-mentioned protocol. The studies were performed using freshly grown bacterial

cultures having an initial cell density of 10^7 CFU/mL. The concentrations of the antimicrobials were varied between IC_{50} and $10\times IC_{50}$ and the treatment timings were kept as 6, 12, 24 and 48 h.

FACS analyses

For the estimation of viable and dead cells, FACS studies were performed as follows: The antimicrobial-treated bacterial cultures were pelleted down at 5000× g for 10 min and then washed with 0.9 % NaCl. After which, the cells were stained using the commercially procured kit, from which 2 μL of SYTO9 and 1 μL of PI were incubated in the dark for 1 h to stain the live and dead cells, respectively.[3] The stained cells were centrifuged once again at 5000× g for 10 min, and the obtained pellet was washed once with 0.9 % NaCl and then used for analysis. Three controls, such as live, dead and unstained cells, were used as references, for which the dead cells were obtained by treating them with 70% isopropanol. The concentrations of UGN(-)GSH and UGN(+)GSH50 were taken as IC_{50}, $2\times IC_{50}$, $4\times IC_{50}$ and $8\times IC_{50}$, beyond which no significant cell pellet could be obtained, possibly due to severe cell damage and hence limited to this concentration range.

Experimental evolution of resistance

To determine any resistance development, the ancestor populations were subjected to 30 passages by periodic exposure to IC_{50} concentrations of UGN(-)GSH and UGN(+)GSH50. Untreated cells were used as controls. The passaging was performed with 1.5 mL solution containing 10^7 CFU/mL bacterial cells that was treated with an equivalent volume of the solution containing the antimicrobial substance.[4] The resultant mixture was incubated for 3 h at 37 °C, following which the cells were subjected to centrifugation at 5000× g for 10 min at 4 °C. The obtained pellet was resuspended in 1 mL of media, from which 500 μL was transferred to 2.5 mL of fresh media and incubated overnight. After the OD_{600} of the solution crossed 2.0, a portion of the cultures was diluted to a cell density of 10^7 CFU/mL and used in the next passage. One lineage was developed against each of the antimicrobial such as UGN(-)GSH, UGN(+)GSH50 and ampicillin and the resazurin assay to determine the IC_{50} was performed in duplicate in this case.

Gold quantification using ICP-OES

About 200 μL of the ancestor and resistant bacterial populations were treated for 6 h with their respective $2\times IC_{50}$ concentrations (200 μL) of UGN(-)GSH and UGN(+)GSH50. The treated cells were then subjected to centrifugation at 5000× g for 10 min to separate the pellets from the supernatant. The gold present in both pellets and supernatant solutions was dissolved in 1 mL and 600 μL of aqua regia, respectively, to which additional 5 mL of 10% HCl was added prior to the gold quantification through inductively coupled plasma optical emission spectroscopy (ICP-OES).[5]

Next-generation sequencing (NGS) analysis

The populations subjected to the passaging studies with antimicrobials up to 30 days were employed for genomic DNA isolation using phenol-chloroform method.[6] A control population passaged in a similar fashion but without subjecting to any antimicrobial exposure was also included. The extracted genomic DNA was subjected to whole genome sequencing, for which the paired-end sequencing libraries were prepared from the DNA samples using the Illumina TruSeq Nano DNA Library Prep kit. The high-quality reads of the obtained variant sequences were aligned to the reference genome (*E. coli* K-12 MG1655 database available from the National Center for Biotechnology Information (NCBI)) using BWA MEM (version 0.7.17) for the identification of mutations. The occurred mutations (100% frequency) were identified by aligning with the sequences from the coding regions against those of the ancestor and control populations. To analyze the affected biological, cellular and molecular functions due the mutant genes in each category, KEGG enrichment analysis was conducted using Partek® Genomics Suite® (version:7.18.0723). The GO enrichment analysis was carried out to identify statistically enriched categories in the mutant genes with a significant threshold p-value of <0.05. The gene function was

identified manually from the NCBI gene database for the functional categorization of all the mutations (http://www.ncbi.nlm.nih.gov/gene). For the specific pathway analysis, a dataset containing mutated genes was uploaded to STRING database (version 11.0b, https://string-db.org/). The significantly enriched KEGG pathways were determined with the default parameter settings (with full STRING network, medium confidence score > 0.4 and FDR stringency of less than 5%).

Reactive oxygen species (ROS) studies

About 150 μL of the ancestor and resistant populations of the bacterial cells having a cell density of 10^7 CFU/mL were individually treated with 30 μL of 50 μM DCFH-DA and incubated for 1 h at 37 °C in the dark under 200 rpm shaking to facilitate the dye internalization by the cells.[7,8] Subsequently, 150 μL of the solutions containing UGN(-)GSH and UGN(+)GSH50 were added to the bacterial cells at their respective IC_{50} concentrations, which were then incubated for 6 h. Following this, the solutions were subjected to centrifugation at 2000 rpm for 2 min and the fluorescence intensity of the supernatant solutions was measured. It can be noted that DCFH is not a specific probe to any particular ROS and thus quantifies the overall reactive species. The stability of this probe was ascertained through a control study up to 6 h, as DCFH-DA is sensitive to local pH and oxygen levels.[9]

RT-qPCR studies

The primers for *narJ* gene were designed to probe the response to the oxidative stress, while *gyrB* was employed as the house keeping gene. Complete gene sequences were retrieved from the NCBI database and the primers were designed using the Primer 3.0 online software. The parameters such as melting temperature (T_m) and % GC content were tightly regulated below 65 °C and <60%, respectively.

Initially, RNA isolation was performed using the trizol method for RT-qPCR studies.[10] For this, about 2.5 mL of the bacterial cultures was employed and treated with the antimicrobials at IC_{50} concentrations for 6 h, followed by pelleting down the cells by centrifuging at 5000× *g* for 10 min at 4 °C. The isolated RNA was dissolved in 40 μL of nuclease-free water, incubated at 55 °C for 15 min and then quantified with nano-drop reading and 1.2% agarose gel. Further cDNA conversion was performed using PrimeScript 1st strand cDNA Synthesis Kit (Takara). Using this cDNA, RT-qPCR experiments were performed following the standard protocol using the TB green kit (Takara).

Supplementary figures and discussion
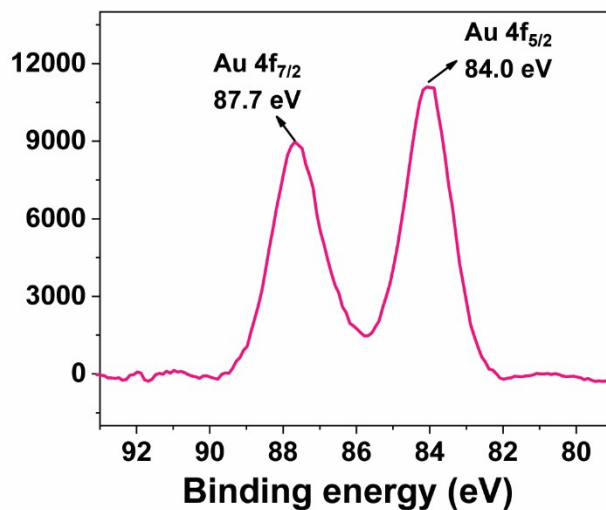
Fig. S1. XPS narrow scan spectrum of Au 4*f* depicting the zerovalent nature of gold in the as-synthesized Au NCs.
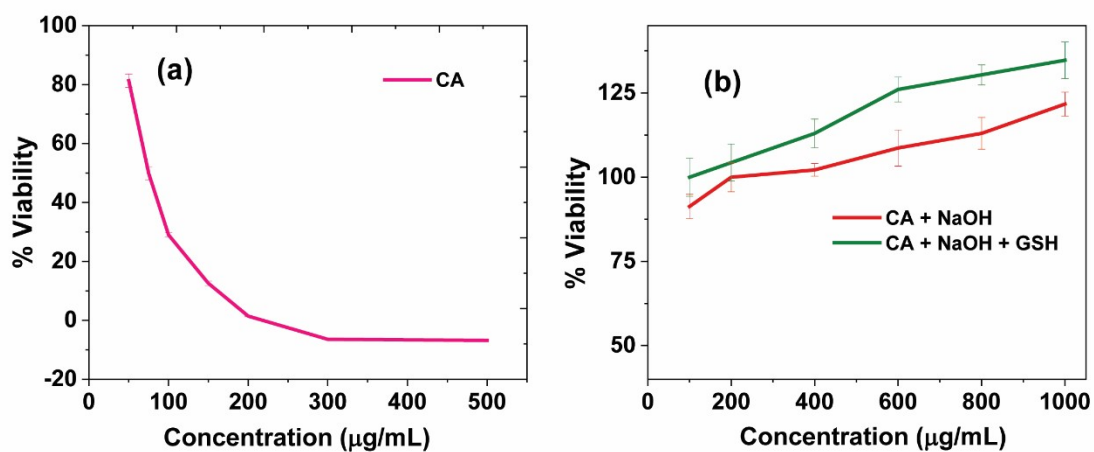
Fig. S2. Viability studies using resazurin assay against (a) pristine CA and (b) CA neutralized with NaOH and the same with GSH addition.

Surface ligand modulation of the UGNs

The modulation of the surface-active sites was probed by 2-MBI method using LC (Fig. S3).[1] The LC measurements showed that the surface active sites on the UGN(-)GSH and UGN(+)GSH50 experienced a slight decline in coverage compared to the as-synthesized NCs. This is indicative of a small degree of aggregation or particle growth, resulting in the loss of active sites to a little extent. However, a higher GSH content of 100% and 200% resulted in significantly lesser amount of 2-MBI probe binding to the gold surface, indicating the higher surface coverage by the pre-existing GSH.
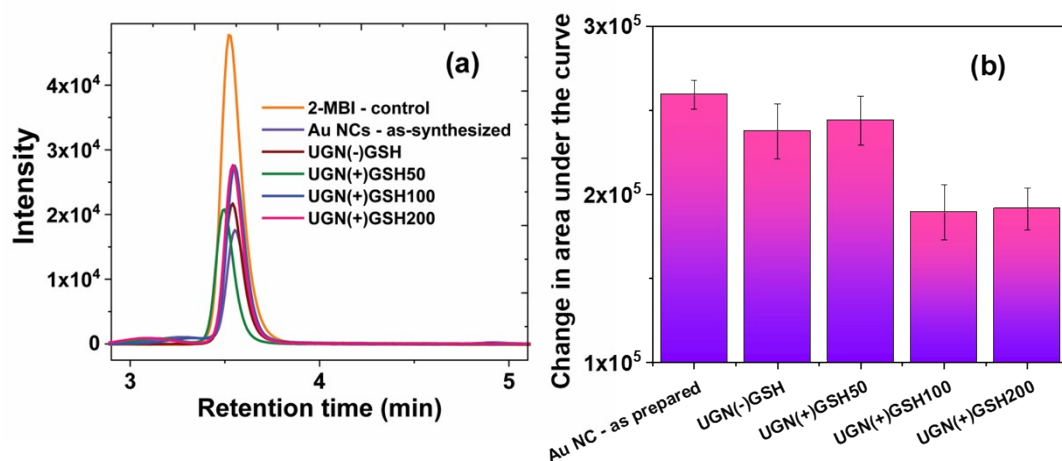
Fig. S3. 2-MBI adsorption on UGNs shown through liquid chromatography profiles (a) and changes in 2-MBI's area under the curve (b).

To gain further insights into the surface coverage of UGNs with GSH, we additionally conducted proton nuclear magnetic resonance (^{1}H NMR) spectroscopic studies using D_2O solvent (Fig. S4). A solution of 2 mg GSH in 0.5 mL of D_2O yielded a well-resolved spectrum, whose characteristic signals were found to agree with the established structure. On the other hand, when GSH-capped ultrafine gold nanosystems (UGNs) were subjected to NMR analyses, the characteristic signals of GSH were not observed and the spectra mostly resembled to that of UGN(-)GSH, wherein only the peaks correspond to citrate matrix were visible. It can be noted that the amount of GSH taken in UGN(+)GSH100 was equal to that employed in the pristine GSH sample. However, when the GSH content was increased to 200% (i.e., 2 times higher than the control sample), small degrees of broad signals corresponding to GSH were observed. These observations may be attributed to the adsorption of GSH over the UGNs. It can be found from the literature that the J-coupling (splitting) of GSH protons was not visible after its binding in atomically-precise UGNs, which indicates a compromise in the resolution.[11] Thus, we speculate that the disappearance of the characteristic signals of GSH in the UGNs could be attributed to the compromised sensitivity due to binding over the surface of UGNs. When the GSH content was further increased to the mass equivalent of citric acid, intense and well-resolved signals from GSH were detected. Nevertheless, the chemical shift values of the protons in citrate and GSH—in comparison to the pristine samples—were found to be shifted, indicating the interaction between these two components. Hence, there could be a certain influence from the citrate matrix, which warrants additional study to shed more light into deeper insights on the observations. Assuming the loss in GSH signals is mainly due to the binding of GSH over UGNs, the higher stoichiometry of GSH in UGN(+)GSH200 can be attributed to the multiple Au–S ligations at the surface.[1] Such a higher stoichiometric binding of thiolated ligand was also experimentally shown by Fernandez et al. through extended X-ray absorption-fine structure (EXAFS) studies.[12]
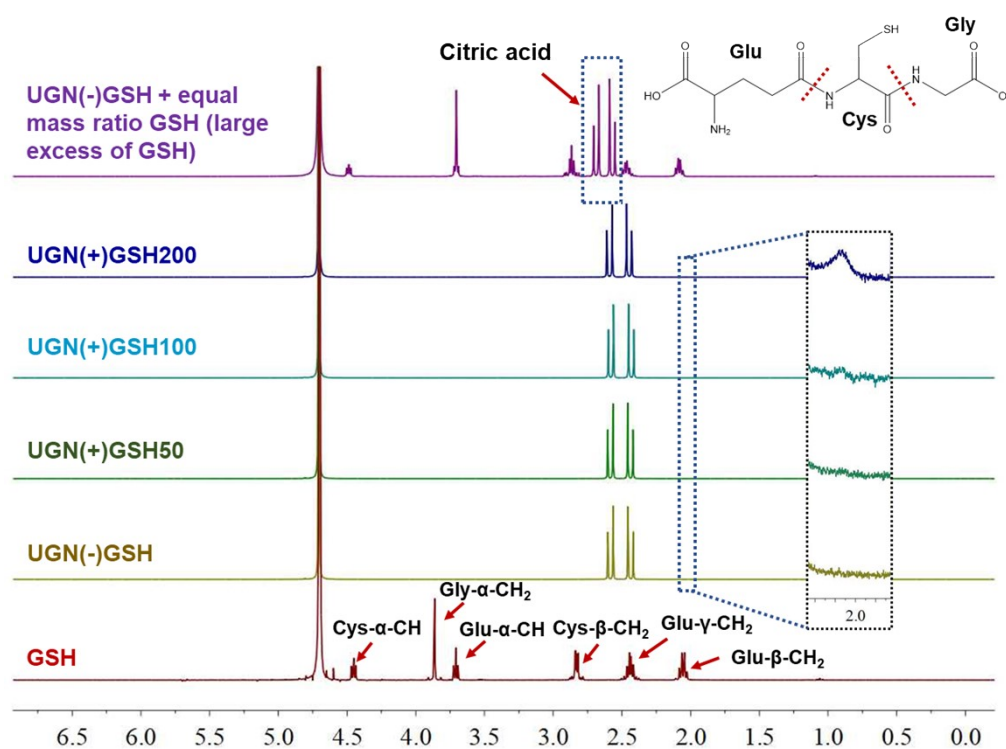
Fig. S4. Proton nuclear magnetic resonance (^{1}H NMR) spectra of GSH-capped UGNs in comparison to non-GSH-capped UGNs, pristine GSH and non-GSH-capped UGNs added with equal mass ratio of GSH. The magnified region corresponding to the Glu-β-CH$_2$ protons in the UGNs has been shown in the inset.
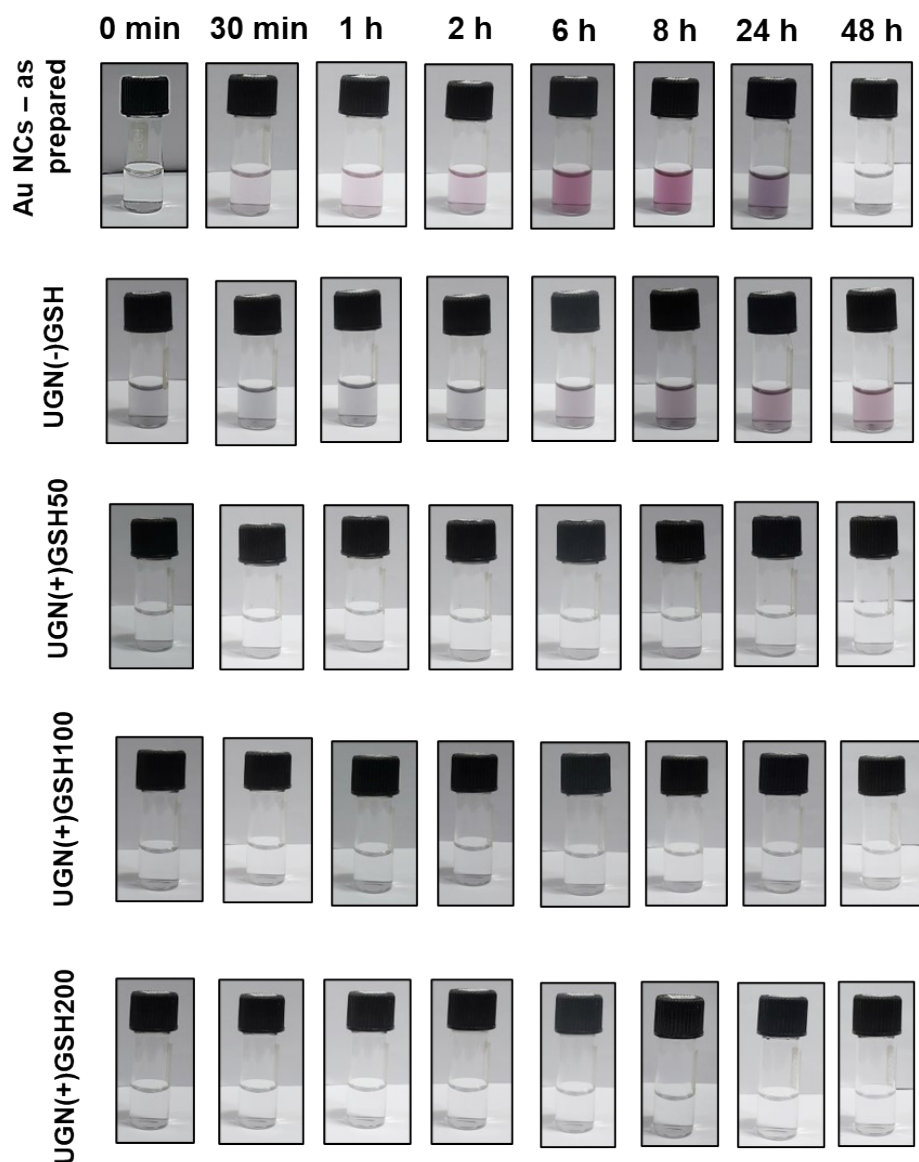
Fig. S5. Digital photograph (corresponding to the graphs shown in Fig. 1(e–i)), taken at different time intervals, depicting the stability analysis of non-GSH capped and GSH-capped UGNs in comparison to the as-synthesized ones. The concentration of the samples employed was 3 mg/mL in each case.
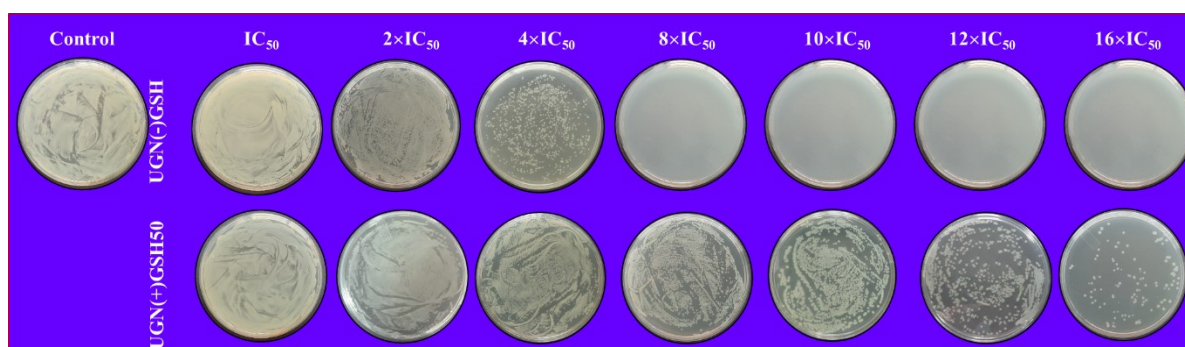
Fig. S6. Minimum bactericidal concentration (MBC) studies by treating the cultures with different concentrations of UGNs for 6 h, followed by incubation for 24 h in agar plate.

ROS generation studies

As ROS produced by the Au nanosystems is known to be an important mechanism in eliciting antimicrobial properties, its generation studies were conducted using the DCFH-DA assay to compare the levels of oxidative stress in resistant populations after 30 passages with those in ancestor populations, following treatment with the UGNs (Fig. S7(a)).[13] While the ancestor populations treated with ampicillin and UGN(+)GSH50 did not show any significant elevation in ROS generation level, the same treated with UGN(-)GSH showed about 1.4 fold increase in the ROS level, compared to the untreated controls. On the other hand, the resistant populations treated with ampicillin and UGN(+)GSH50 exhibited ~3-fold increase in the ROS generation, whereas ~6-fold increase in the same was shown by the resistant populations treated against UGN(-)GSH. These results can be correlated to the burst activity and steady-but-sustained activity of non-GSH-capped and GSH-capped UGNs, respectively. Furthermore, the higher fold-increase in the ROS generation in the resistant population could be attributed to the requirement of higher oxidative stress level to elicit a similar magnitude of antimicrobial activity in the ancestor population.

RT-qPCR analysis of *narJ* expression level

To reinforce the findings from the DCFH-DA assay investigations, RT-qPCR studies were carried out to assess the expression levels of *narJ* gene—associated with the oxidative stress—in both the ancestral and resistant populations (Table S3). The obtained results were analyzed using the $2^{-\Delta\Delta CT}$ method and presented in Fig. S7(b). It can be noted that *narJ* gene plays a major role in respiratory nitrate reduction, generating protonmotive force through nitrate-quinol redox reactions.[14] Thus, it helps in the process of energy generation and protects the cells from oxidative stress. In the ancestor populations, the expression levels of *narJ* gene was modestly downregulated in the ampicillin and UGN(+)GSH50 treatment cases, whereas a very gentle upregulation was observed in the case of UGN(-)GSH. This observation was in agreement with the ROS generation assessment by the DCFH-DA assay. In the case of resistant populations, the *narJ* gene expression level was found to be significantly upregulated, particularly in the UGN(-)GSH and UGN(+)GSH50 cases. The highest expression level with UGN(+)GSH50 may be correlated with the higher fold increase in the IC_{50} study (Fig. 4a), though additional studies would be required to ascertain this.

Percentage gold distribution between the cell pellet and supernatant

It is evident from the cell viability studies that the resistant populations required higher amount of the antimicrobials to achieve a similar level of bactericidal activity. Therefore, to gain a deeper understanding of the percentage distribution of gold within a sample, ICP-OES analysis was conducted on both ancestor and resistant populations. This method allowed for examining the amount of gold in the cell pellet and the supernatant, providing valuable insights into its distribution (Fig. S7(c)). The results showed two key findings: (i) Compared to the GSH-capped ones, the samples treated with non-GSH-capped UGNs displayed a higher gold content in the pellet, likely due to their lesser stability, leading to an indiscriminate attack over the cells. In the case of GSH-capped UGNs, the steady-but-sustained activity elicited a similar antibacterial activity with a relatively lesser amoung of gold uptake. (ii) Both ancestor and resistant strains had a comparable percentage distribution of gold between the pellet and supernatant, with the pellet having a slightly more gold content than the ancestor populations.
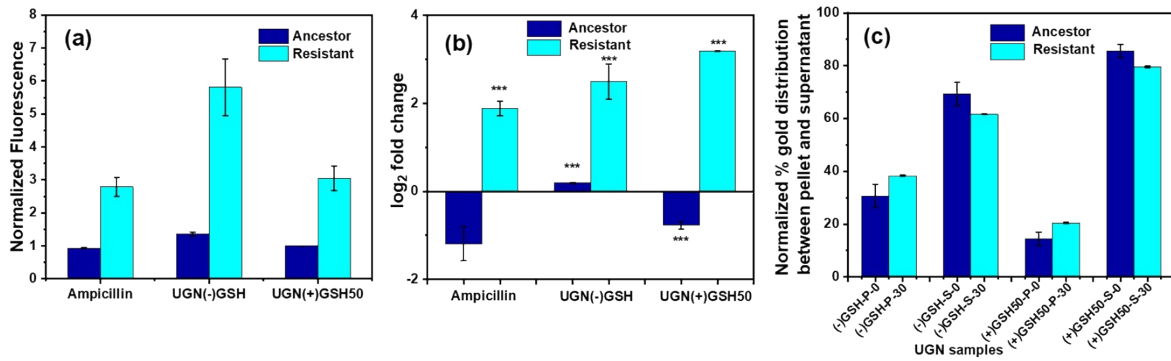
Fig. S7. Normalized plots in triplicates (with respect to the untreated control populations) depicting oxidative stress assessment using **(a)** ROS generation and **(b)** RT-qPCR on *narJ* gene expression levels in the ancestor and resistant populations against different antimicrobials employed in the study. The p values in the statistics are applied as follows: $p <= 0.001$ is most significant (***), $p <= 0.01$ and >0.001 is more significant (**) and $p <= 0.05$ and >0.01 is significant (*)). **(c)** ICP-OES measurements in duplicate for gold quantification in the cell pellet (represented by 'P') and supernatant (designated as 'S') of the populations treated with UGNs. The numbers 0 and 30 in the sample codes represent the bacterial cultures from the 0th and 30th cycles of the passaging studies, respectively.
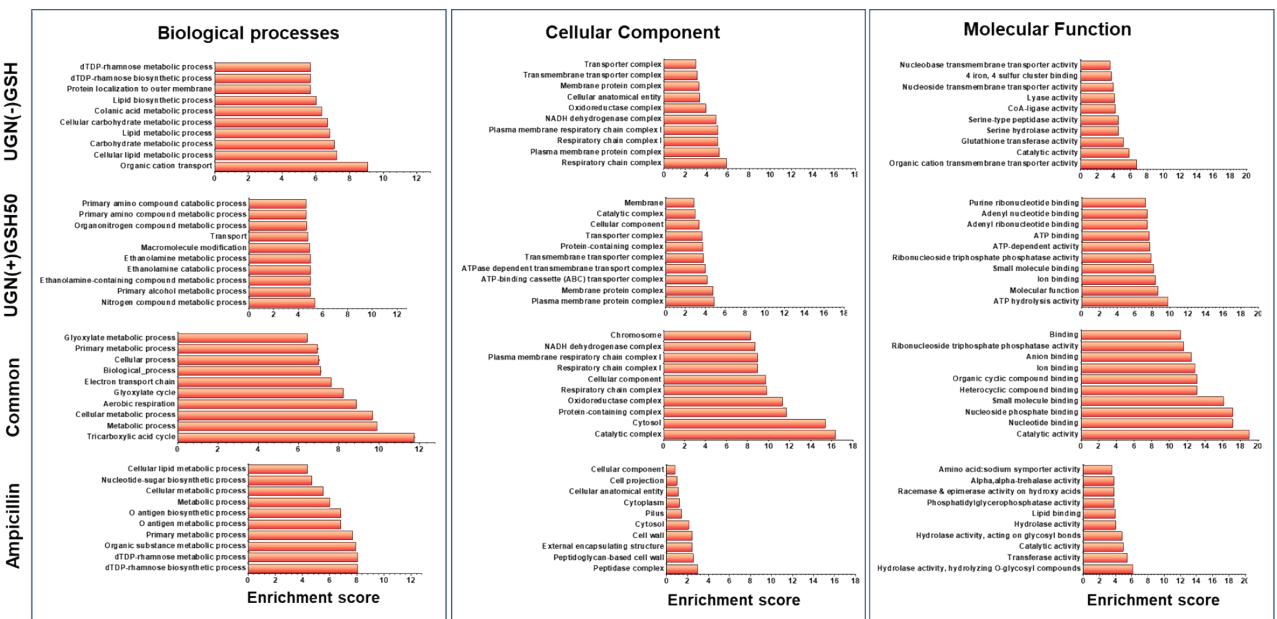
Fig. S8. The pattern of mutations in antimicrobial-resistant populations categorized through GO analyses of the mutations in antimicrobial resistant populations for the biological processes, cellular component and molecular function. The analyses are sorted based on mutations that are common to both UGN(-)GSH and UGN(+)GSH50, as well as those specific to each antimicrobial.
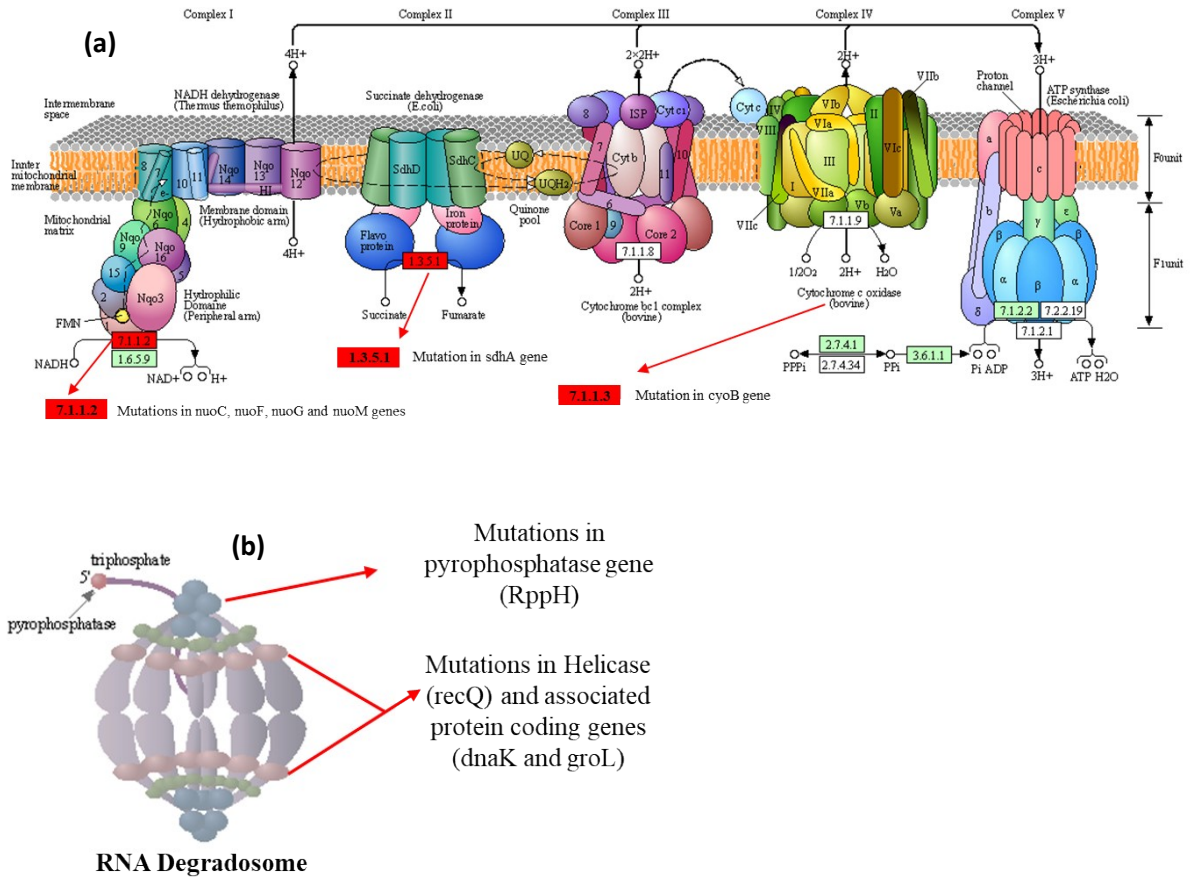
Fig. S9. Genes impacted in the (a) oxidative phosphorylation (highlighted in red) and (b) RNA degradation processes.
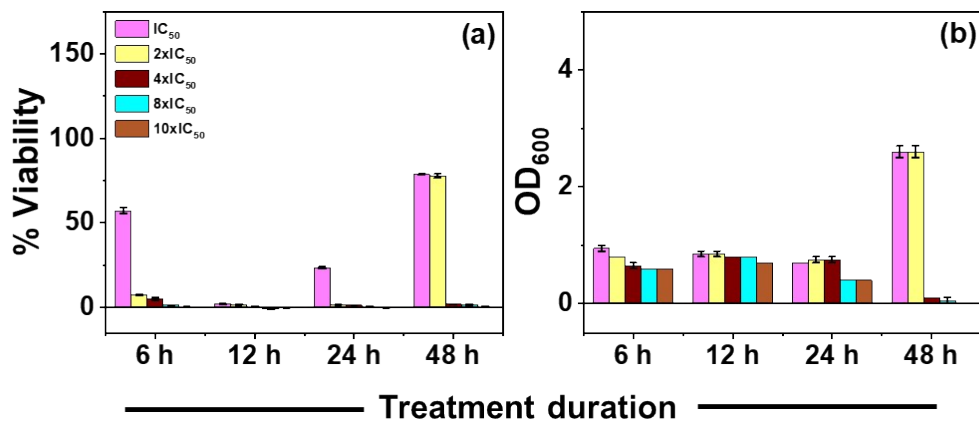
Fig. S10. Resuscitation studies using (a) Resazurin assay and (b) OD_{600} measurements of the bacterial cultures against different concentrations of UGN(+)GSH100.

Supplementary Tables

Table S1. Particle size analysis through DLS measurements. The particle size details from two major peaks are presented. The measurements were performed in triplicate, with 30 scans per measurement and the results are presented as averages.

Sample	Peak	DLS (d, nm)	% Volume	Std. deviation (nm)	Zeta potential (mV)	Std. deviation (mV)
As-synthesized Au NCs 1 mg/mL in water	1	6.96	97.1	1.76	-5.76	0.30
	2	41.22	2.9	25.74		
As-synthesized Au NCs 1 mg/mL in media	1	10.27	99.8	6.62	-10.44	0.56
	2	4921	0.2	923.2		
UGN(-)GSH ($2 \times$ IC$_{50}$) in media	1	27.89	76.6	11.18	-14.23	0.54
	2	788.9	13.4	215.1		
UGN(+)GSH50 ($2 \times$ IC$_{50}$) in media	1	14.04	90.8	3.45	-14.20	0.71
	2	76.74	9	36.06		

Table S2. Comparison of IC$_{50}$ and MIC values obtained from the resazurin assay and broth dilution method, respectively.

Antimicrobial compound	0th day		30th day	
	IC$_{50}$	MIC	IC$_{50}$	MIC
Ampicillin (μM) (μg/mL†)	1 (0.35)	2 (0.7)	13.4 (4.7)	25 (8.8)
UGN(-)GSH (μg/mL)	8.3	8.3	27.0	24.9
UGN(+)GSH50 (μg/mL)	8.3	16.6	30.2	33.2

†**Footnote:** The values shown in the bracket for Ampicillin are in μg/mL.

Table S3. Primers employed in the RT-qPCR studies, where *gyrB* was chosen as the housekeeping gene.

Gene	Primer	Forward/ Reverse	Melting point (T$_m$) (°C)	GC content (%)
gyrB	5' CAACAACATTCCGCAGCGTG 3'	Forward	61.00	55.0
gyrB	5' CAACCGCCGATTTCACCTCA 3'	Reverse	60.95	55.0
narJ	5' TTCCTGCGCGATTTAACGGC 3'	Forward	61.97	55.00
narJ	5' CCGGTAATTCGCGGCTGTTT 3'	Reverse	61.64	55.00

Table S4. KEGG pathway analysis through the STRING tool of the mutated genes.

KEGG Pathway ID	Description	Observed gene count	Background gene count	Strength	False discovery rate (FDR)	Mutated genes
eco01100	Metabolic pathways	30	890	0.32	0.0018	*carB, araB, acnB, dapD, fadE, betB, cyoB, nagB, sdhA, putA, purB, icd, puuB, dcd, napA, nuoM, nuoG, nuoF, nuoC, purL, gabD, glcD, yiaY, mtlA, ilvD, fadB, ppc, aceA, phnJ, rsgA*
eco00190	Oxidative phosphorylation	6	43	0.94	0.0057	*cyoB, sdhA, nuoM, nuoG, nuoF, nuoC*
eco03018	RNA degradation	4	16	1.19	0.0085	*dnaK, rppH, recQ, groL*

Table S5. Time-kill MBC studies employing different concentrations of UGN(-)GSH and UGN(+)GSH50.

Antimicrobial UGN	Duration	IC_{50}	$2 \times IC_{50}$	$4 \times IC_{50}$	$8 \times IC_{50}$	$10 \times IC_{50}$	$12 \times IC_{50}$	$16 \times IC_{50}$
UGN(-)GSH	6 h	+++	+++	++	-	-	-	-
	12 h	+++	+++	++	-	-	-	-
	24 h	+++	+++	+++	+++	+++	++	+
	48 h	+++	+++	+++	+++	+++	+++	++
UGN(+)GSH50	6 h	+++	+++	+++	+++	+++	++	+
	12 h	+++	+++	+++	++	++	+	-
	24 h	+++	+++	+	-	-	-	-
	48 h	+++	+++	+++	+++	+++	-	-

Footnote: Notations followed for the bacterial growth: (+++) Confluence; (++) medium; (+) below-moderate; (-) no growth.

References

1. D. Patra, S. R. Nalluri, H. R. Tan, M. S. M. Saifullah, R. Ganesan and B. Gopalan, *Nanoscale Advances*, 2020, **2**, 5384-5395.
2. H. Mude, P. A. Maroju, A. Balapure, R. Ganesan and J. Ray Dutta, *Food Chemistry*, 2022, **374**, 131830.
3. C. Hobson, A. N. Chan and G. D. Wright, *Chemical Reviews*, 2021, **121**, 3464-3494.
4. H. Mude, P. A. Maroju, A. Balapure, R. Ganesan and J. Ray Dutta, *ACS Applied Bio Materials*, 2021, **4**, 8396-8406.
5. M. Midhu Francis, A. Thakur, A. Balapure, J. Ray Dutta and R. Ganesan, *Chemical Engineering Journal*, 2022, **446**, 137363.
6. J. Zeng, Z. Guo, Y. Wang, Z. Qin, Y. Ma, H. Jiang, Y. Weizmann and X. Wang, *Nano Research*, 2022, **15**, 4164-4174.
7. Z. Cao, J. Chen, J. Tran, X. Chen, B. Bacacao, L. A. Bekale and P. L. Santa Maria, *ACS Applied Bio Materials*, 2020, **3**, 5275-5286.

8. E. M. Higbee-Dempsey, A. Amirshaghaghi, M. J. Case, M. Bouché, J. Kim, D. P. Cormode and A. Tsourkas, *Journal of the American Chemical Society*, 2020, **142**, 7783-7794.
9. K. Zheng, M. I. Setyawati, D. T. Leong and J. Xie, *ACS Nano*, 2017, **11**, 6904-6910.
10. G. B. Hwang, H. Huang, G. Wu, J. Shin, A. Kafizas, K. Karu, H. D. Toit, A. M. Alotaibi, L. Mohammad-Hadi, E. Allan, A. J. MacRobert, A. Gavriilidis and I. P. Parkin, *Nature Communications*, 2020, **11**, 1207.
11. Z. Wu, C. Gayathri, R. R. Gil and R. Jin, *Journal of the American Chemical Society*, 2009, **131**, 6535-6542.
12. P. Crespo, R. Litrán, T. C. Rojas, M. Multigner, J. M. de la Fuente, J. C. Sánchez-López, M. A. García, A. Hernando, S. Penadés and A. Fernández, *Physical Review Letters*, 2004, **93**, 087204.
13. Y. Xie, Q. Zhang, W. Zheng and X. Jiang, *ACS Applied Materials & Interfaces*, 2021, **13**, 35306-35314.
14. P. Ceccaldi, J. Rendon, C. Léger, R. Toci, B. Guigliarelli, A. Magalon, S. Grimaldi and V. Fourmond, *Biochimica et Biophysica Acta (BBA) - Bioenergetics*, 2015, **1847**, 1055-1063.